Hydrogenation Catalysis

Deutsche Ausgabe: DOI: 10.1002/ange.201603332
Internationale Ausgabe: DOI: 10.1002/anie.201603332

Controlling Ethylene Hydrogenation Reactivity on Pt_{13} Clusters by Varying the Stoichiometry of the Amorphous Silica Support

Andrew S. Crampton, Marian D. Rötzer, Florian F. Schweinberger, Bokwon Yoon, Uzi Landman, and Ueli Heiz**

Abstract: *Ethylene hydrogenation was investigated on size-selected Pt_{13} clusters supported on three amorphous silica (a-SiO_2) thin films with different stoichiometries. Activity measurements of the reaction at 300 K revealed that on a silicon-rich and a stoichiometric film, Pt_{13} exhibits a similar activity to that of Pt(111), in line with the known structure insensitivity of the reaction. On an oxygen-rich film, a threefold increased rate was measured. Pulsing ethylene at 400 K, then measuring the activity at 300 K, resulted in complete loss of activity on the silicon-rich surface compared to only marginal losses on the other surfaces. The measured reactivity trends correlate with charging characteristics of a Pt_{13} cluster on the SiO_2 films, predicted through first-principle calculations. The results reveal that the stoichiometry-dependent charging by the support can be used to tune the selectivity of reaction pathways during a catalytic hydrogenation reaction.*

Model catalysis on supported transition-metal particles under ultrahigh-vacuum (UHV) conditions allows precise control of critical factors that govern heterogeneously catalyzed reactions, thereby reducing the complexity of the system and allowing targeted investigations of key parameters influencing the reaction activity, selectivity, and specificity of a catalyst.[1–3] To date, UHV studies have shown the ability to influence the chemical and/or morphological properties of nanoparticles supported on thin metal oxide films[4] by controlling the precise particle size,[5–9] the film thickness,[10–15] the presence of defect sites,[4,6,16] and the reduction state of the thin film.[17]

A commonly used support in heterogeneous catalysis is a-SiO_2,[18,19] and it has been shown that a-SiO_2 thin films grown in UHV provide an opportunity to vary the metal oxide stoichiometry through selection of the growth parameters.[20] In particular, early experiments demonstrated three types of a-SiO_2 films that can be grown under UHV conditions on a metal single crystal: silicon-rich, stoichiometric, and oxygen-rich; initial investigations showed no differences in their interaction with adsorbed silver atoms.[21] The silicon-rich a-SiO_2 film represents a support which has electron-donating properties; that is, the surface is expected to donate electronic charge to the deposited metal clusters.[22] The platinum clusters on the stoichiometric film are expected to remain charge-neutral overall, whereas the oxygen-rich surface is expected to deplete electronic charge from the deposited Pt clusters (that is, partial positive charging), as is the case for platinum adsorbed on oxide surfaces.[23]

Identification, characterization, and understanding of the factors that govern the reactivity and selectivity of catalytic reactions is complicated by the multiplicity of parameters that need to be considered. These include: structural aspects (pertaining to atomic-scale geometrical arrangements of the adsorbed metal particle, the supporting surface, and the adsorbed reactants), electronic spectra and substrate-induced effects (for example, support-mediated catalyst-particle charging), and size-effects that influence the aforementioned factors, as well as underlie the classification of heterogeneous catalytic reactions into size/structure dependent or independent reactions.

Fundamental insight into these reactivity-controlling factors can be enhanced through research strategies that allow deconvolution of at least some of the above-noted interdependent effects. This is indeed the approach that we have taken in this work by using the aforementioned stoichiometrically different SiO_2 films used as support surfaces, and by exploiting our capability of performing reactivity studies on single-sized catalysts particles (Pt_{13} in this study). This allows for an unparalleled degree of complexity reduction, as only a single parameter in the catalyst system is being varied (namely, the support surface stoichiometry), keeping unchanged the chemical identity of the substrate and the supported metal clusters, the size of the catalyzing particles, and the experimental conditions.

Ethylene hydrogenation on platinum is a classical model heterogeneous catalytic reaction for hydrocarbons, which has been extensively investigated on a variety of metal oxide supported particles, as well as single crystals.[24–29] This reaction has been customarily classified as structure-insensitive, that is the activity does not change with particle size, or

[*] Dr. A. S. Crampton, M. D. Rötzer, Dr. F. F. Schweinberger, Prof. Dr. U. Heiz
Technische Universität München
Lehrstuhl für Physikalische Chemie
Zentralinstitut für Katalyseforschung und Fakultät für Chemie
Ernst-Otto-Fisher-Strasse 1 und Lichtenbergstrasse 4
85747 Garching (Germany)
Dr. B. Yoon, Prof. Dr. U. Landman
School of Physics, Georgia Institute of Technology
Atlanta, GA 30332-0430 (USA)
Dr. A. S. Crampton
Current Address: Harvard University
Department of Chemistry and Chemical Biology
12 Oxford St., Cambridge, MA 02138 (USA)

Supporting information for this article (experimental procedures for film growth, activity measurements, and SiO_2 characterization data, along with computational methods for the a-SiO_2 film and Pt_{13} cluster) can be found under: http://dx.doi.org/10.1002/anie.201603332.

single crystal facet. However, a recent reassessment has concluded against the applicability of such classification for platinum catalyst particles of sub-nanometer dimensions. This was shown in a joint theoretical and experimental approach to coincide with the suppression of ethylene dehydrogenation on Pt_{13}, which induces structure insensitivity, at low temperature (<400 K).[30,31] Consequently, we focus in this work on ethylene hydrogenation turnover frequencies (TOF) on a single cluster size (Pt_{13}) supported on the aforementioned a-SiO_2 supports grown on a Pt(111) single crystal and isolate the effect of support stoichiometry on the reaction activity, as well as demonstrate that the stoichiometry can be used to tune the activity of the reaction.

A UHV chamber equipped with a laser vaporization cluster source[32] was used to synthesize three different a-SiO_2 thin films on a Pt(111) single crystal using the procedure detailed in our previous publication.[33] These films (which are 4–5 layers thick) are: silicon-rich, stoichiometric, and oxygen-rich. Complete experimental details of the film growth, characterization, cluster deposition, and activity measurements can be found in the Supporting Information. Figure 1 a shows the TOF of Pt_{13} at 300 K (blue) as a function of the a-SiO_2 support stoichiometry measured using a pulsed molecular beam technique (PMB),[34,35] along with the TOF measured at 300 K but after pulsing a defined amount of ethylene at an elevated temperature of 400 K (green). Also included for comparison are the results obtained by performing the same experiment on a Pt(111) single crystal. There is a distinct reactivity trend before and after the 400 K step, which correlates with the support stoichiometry. The Pt_{13} clusters on both the silicon-rich and stoichiometric film exhibit at 300 K a similar activity to the Pt(111) single crystal, whereas the oxygen-rich film activity shows an almost threefold increase. After pulsing a defined amount of ethylene at an elevated temperature of 400 K, the TOFs measured again at 300 K (green) show that the clusters supported by the silicon-rich film exhibit a total deactivation, while those on the oxygen-rich film lose about half their activity. The clusters supported on the stoichiometric film show almost no deactivation, while the Pt(111) single crystal loses some activity.

IR reflection absorption spectra (IRRAS) of CO adsorbed on the clean Pt_{13} clusters and after the deactivation step are displayed in Figure 1 b. The clusters adsorbed on the oxygen-rich and stoichiometric film both show a red-shift after the deactivation step, while on the silicon-rich film no signal is observed.

Insights into the experimentally measured dependencies of the hydrogenation and dehydrogenation reactions on the stoichiometry of the a-SiO_2 support were obtained through first-principles simulations of the structural and electronic characteristics of Pt_{13} clusters adsorbed on an a-SiO_2 surface. This substrate has been specifically designed as a four-layer-thick (on average) film deposited on a Pt(111) surface, aiming at simulating the films used in the experiments (see the Supporting Information for experimental characterization of the films). Combined classical molecular dynamics and quantum-mechanical (density-functional theory, DFT) simulations have been used in preparing these films (see the

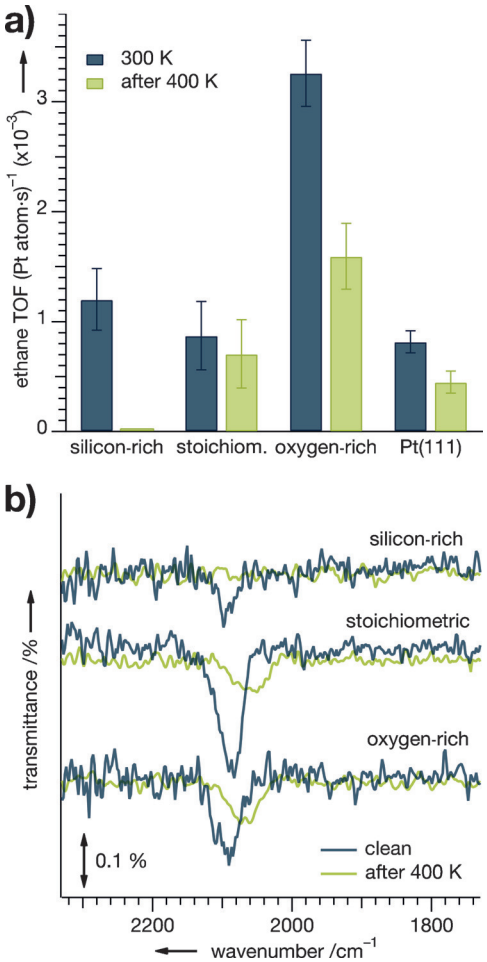

Figure 1. Ethylene hydrogenation kinetic data and IRRAS results with CO as a chemical probe before and after reaction. a) Pt_{13} TOF at 300 K as a function of SiO_2 support stoichiometry before (blue) and after (green) pulsing at 400 K. b) IRRAS of CO from the cluster samples before (blue) and after (green) the complete cycle in (a).

Supporting Information). In Figure 2 we display results from DFT calculations for two structural motifs of the adsorbed Pt_{13} clusters: one comprised of a two-layer structure (with 7 Pt atoms in the bottom layer, and 6 atoms on top; a similar bilayer structure of Pt_{13} on alumina has also been previously reported),[36] and the other having a pyramidal structure; in both cases the structures of the adsorbed clusters have been relaxed with no constraints using DFT-based structural optimizations (see the Supporting Information); the results shown below for both cluster motifs exhibit similar trends. We obtained these results by shifting the position of the Pt_{13} cluster on the surface, thereby generating an ensemble of scanned alternative adsorption sites of the cluster deposited on the surface of the simulated a-SiO_2 substrate; although the a-SiO_2 film has been prepared as a (nominal) stoichiometric film (that is, a film (globally) containing Si and oxygen atoms in the ratio of 1:2), we find that on a local scale it exhibits oxygen-rich and silicon-rich non-stoichiometric regions, along with truly stoichiometric domains.

First we note the large structural heterogeneity of the a-SiO_2 surface reflected in the broad distribution of the total

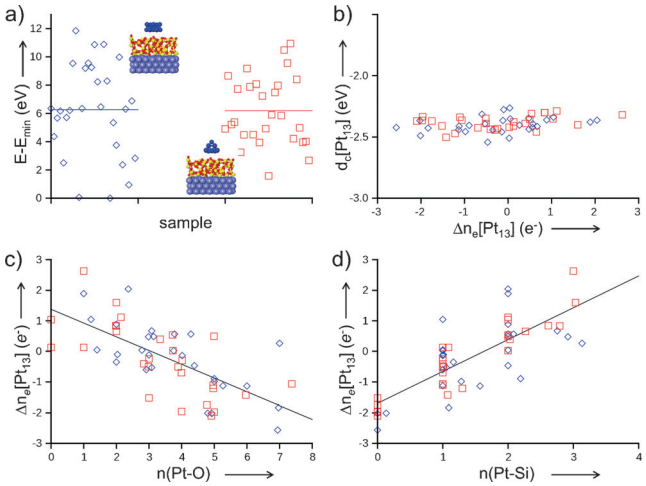

Figure 2. First-principles calculated total energies, d_c (center of the d-electron states), charging of a Pt_{13} cluster supported on a four-layer-thick a-SiO_2 film adsorbed on a Pt(111) surface. Results are shown for two Pt_{13} cluster motifs: a 2-layer structure (blue diamond) and a pyramidal one (red squares); the insets in (a) depict the structures of the two adsorbed platinum clusters (lilac spheres) on the a-SiO_2 film (yellow and red spheres) deposited on a Pt(111) substrate (lilac spheres). The straight lines denote the best fit to the calculated data. a) Total energy distribution of the cluster adsorbed at different sites on the a-SiO_2 surface. Average energies are denoted by horizontal lines. b) The d_c plotted versus the surface-induced electron excess [Δn_e-[Pt_{13}] > 0], or depletion [Δn_e[Pt_{13}] < 0] of the clusters. c) Δn_e[Pt_{13}] plotted vsersus the number of Pt—O bonds formed at the various adsorption sites of the clusters. d) Δn_e[Pt_{13}] plotted versus the number of Pt—Si bonds.

energies of the Pt_{13}/a-SiO_2 clusters calculated at the aforementioned various adsorption sites on the a-SiO_2 surface (Figure 2a), with images of selected optimized adsorbed cluster structures shown in the Supporting Information); these total-energy variations are reflected also in the distribution of the corresponding cluster adsorption energies (see the Supporting Information). In Figure 2b we show the distribution of the d-electron centers (d_c[Pt_{13}]) of the clusters plotted versus the adsorption-induced electron excess [Δn_e-[Pt_{13}] > 0], or depletion [Δn_e[Pt_{13}] < 0] of the clusters, and in Figure 2c,d we display the distributions of Δn_e[Pt_{13}] plotted as a function of the number of bonds made by the adsorbed Pt_{13} cluster to the O and Si atoms of the a-SiO_2 surface (at the various adsorption sites). Importantly, we find that the sign, magnitude, and slope of the extra charge on the clusters (electron excess or depletion) vary in a linear manner as a function of the number of Pt_{13}-to-SiO_2 bonds (n(Pt-O) in Figure 2c and n(Pt-Si) in Figure 2d).

The origins of the observed dependencies of the catalytic TOFs on the cluster charging characteristics discussed above, may be found in the Dewar–Chatt–Duncanson (DCD) donation-back-donation model[37,38] for ethylene adsorption (and hydrogenation/dehydrogenation) on d-electron metals, where donation (back-donation) refer to the interaction of the ethylene π-orbital (π*-orbital) with the metal d-electrons; in the context of the hydrogenation/dehydrogenation reactions these terms signify the (agnostic) interaction between the metal d-electrons and the σ(C-H) (σ(C-H)*) bond of the adsorbed ethylene molecule with the reactant hydrogen atom. These interactions (particularly the back-donation from the metal d-electrons to the antibonding σ(C-H)* orbital) are expected to depend on the charge state of the metal cluster, specifically, the population and location of the highest occupied d-electron states with reference to the Fermi energy.

At this juncture it is pertinent to remark on the lack of dependence of the location of the d-electron centers of the Pt_{13} clusters (d_c, the calculated centroid of the d-electron states) on the charge states of the clusters adsorbed on the a-SiO_2 film (Figure 2b). This reflects the inapplicability for metal clusters of less than about 20 atoms (that is at the bottom of the nanometer size-scale) of d-band model theories,[39] as well as other concepts formulated originally for particles of larger sizes or extended metal surfaces; see a recent reassessment of the validity of the concept of structure sensitivity/insensitivity to sub-nanometer platinum catalysts.[30,31] In this model, a shift in the d_c away from the Fermi level is found to be correlated with lowering of the activation barrier for ethylene hydrogenation, as well as predicting under such circumstances an increase in the activation barrier for ethylene dehydrogenation. In the opposite situation, a shift of the d-band center towards the Fermi level is associated with a lowered activation barrier for ethylene dehydrogenation and an increased barrier for hydrogenation. We have recently observed trends that follow the predictions of the d_c model in studies of the catalyzed hydrogenation of ethylene on larger nanoparticles of Ni, Pd, and Pt supported on MgO(100), where the disposition for catalyst deactivation was directly related to the calculated d-band center of M_{30} (M = Ni, Pd, and Pt) model clusters.[40] The metal with the d-band center closest to the Fermi level, Ni, exhibited the most facile deactivation whereas the metal with a d-band center farthest from the Fermi level, Pt, was most resistant to deactivation.

With these findings we may elucidate the measured reactivity pattern shown in Figure 1a. The silicon-rich a-SiO_2 film donates electron density into the cluster (see Figure 2d), thereby filling unoccupied states closer to the Fermi level. This lowers the barrier for dehydrogenation (activating the process even at 300 K) compared to the stoichiometric film, correlating with our finding (Figure 1a) that only on this support clusters deactivate completely at 400 K. This deactivation is likely caused by a more complete dehydrogenation of ethylene, similar to the species (ethylidyne and graphitic-like) formed on Pt(111) above 450 K upon dehydrogenation of ethylidyne.[41,42] The stoichiometric film shows no deactivation at 400 K, as the next dehydrogenation barrier cannot be overcome at this temperature (in contrast to the aforementioned case of the silicon-rich film) leading to an almost identical activity after the temperature step. The fact that Pt_{13} clusters on the silicon-rich and stoichiometric films exhibit an activity similar to the Pt(111) single crystal surface at 300 K is a strong indication that on these supports ethylene adsorbed on deposited Pt_{13} clusters has already undergone a dehydrogenation step; indeed, it is known that ethylene readily dehydrogenates to form ethylidyne on Pt(111) at these temperatures, and that the hydrogenation reaction proceeds with this species and di-σ- bonded

ethylene as stagnant spectators.[27] This alkylidyne layer has been posited as the reason underlying the structure insensitivity observed for this reaction on platinum.

The oxygen-rich film on the other hand withdraws electrons from the adsorbed clusters; recall the increase in electron depletion, $[\Delta n_e[Pt_{13}] < 0]$, predicted for clusters forming a larger number of Pt–O bonds to the a-SiO_2/Pt(111) surface (Figure 2c). This depletion (which results in a partial positive charge on the cluster) is expected to result in a shift of the d-electron energies away from the Femi level (that is, to more negative energy values). Although no such systematic shift is found for the d-centers calculated for the adsorbed clusters (with the calculated average being $< d_c > = -2.40$ eV regardless of the sign of the surface-induced charge of the cluster; see Figure 2b), we find through an atom-by-atom analysis of the d_c values for charge-depleted clusters ($[\Delta n_e[Pt_{13}] < 0]$) a significant number of atomic sites with their centroid of the d-electron energy levels shifted further away from the Fermi level. This behavior, that serves to illustrate the atom-by-atom heterogeneous behavior of the individual Pt_{13} clusters adsorbed on the a-SiO_2 film, is portrayed by the atomic-scale surface-induced charge (Figure 3a) and atomic d_c distributions (Figure 3b), calculated for a selected partially positively-charged cluster (with $\Delta n_e[Pt_{13}] = -2.6$ e and overall $d_c = -2.42$ eV) bonded to the surface via 7 Pt–O bonds. Such local shifts of the d-electron levels are predicted to bring about increased dehydrogenation activation barriers on Pt_{13} clusters supported on oxygen-rich a-SiO_2 films, compared to the reaction taking place on a-SiO_2 surfaces with other stoichiometries. Consequently, at 300 K the formation of this dehydrogenated product leading to structure insensitivity (tentatively attributed to ethylidyne) has been attenuated. The enhanced activity at 300 K (Figure 1a) is unprecedented as the ethylene hydrogenation is known to be a structure insensitive reaction, as we observe when comparing the other two films to the Pt(111) single crystal. At higher temperatures the first dehydrogenated products start to form on the oxygen-rich support, hence the significant decrease in activity observed after pulsing at 400 K.

Further support for the above interpretation of the reactivity data (Figure 1a) is given by the IRRAS- spectra of CO adsorbed on the supported clusters, measured before and after the complete reaction cycle. After the full reaction sequence displayed in Figure 1a both the oxygen-rich and stoichiometric SiO_2 film show a similar CO stretch frequency (see Figure 1b) which is slightly red-shifted from that of the clean clusters. This red-shift is known to occur when carbon species are co-adsorbed on platinum particles with CO.[43,44] The silicon-rich film shows no CO stretch indicating that the clusters are completely covered by a carbonaceous species within the sensitivity of our experiment. This exemplifies the effect of electron donation into the cluster, namely, increased electron density facilitates the formation of carbon deposits (through dehydrogenation pathways) and quenches the ethylene hydrogenation activity at 300 K.

In summary, focusing on a single cluster size (Pt_{13}) supported on a-SiO_2 surfaces with variable stoichiometry, we have demonstrated the ability to disentangle the effect of the substrate-cluster interactions from other factors that influence the catalyzed ethylene hydrogenation. We have shown that precise control of the support stoichiometry can be used to tune the activity of a catalytic hydrocarbon reaction by suppressing or activating (alternative) side reaction pathways. The proclivity for hydrogenating or dehydrogenating ethylene (Figure 1) was shown to be consistent with partial charging considerations of Pt_{13} clusters

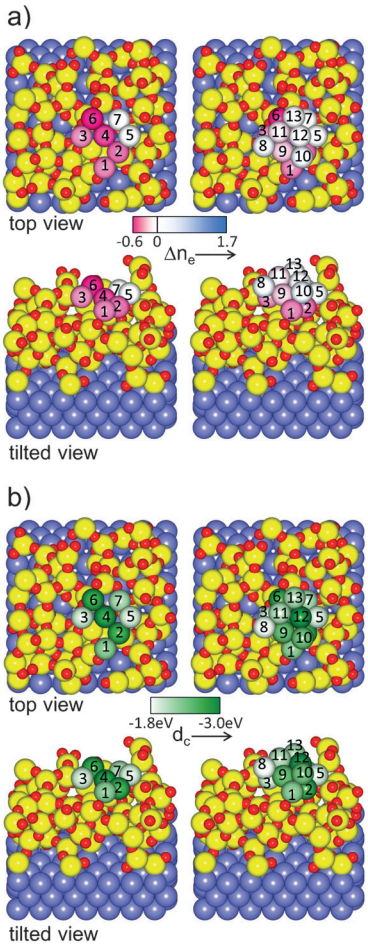

Figure 3. First-principles calculated atomic-scale excess charge Δn_e (a) and d_c-center (b) distributions calculated for a bilayer Pt_{13} cluster supported on a 4-layer thick a-SiO_2 film adsorbed on a Pt(111) surface. The selected adsorbed Pt_{13} cluster is characterized by an overall charge depletion $\Delta n_e[Pt_{13}] = -2.6$ e (positively charged) and $d_c = -2.42$ eV. In each of (a) and (b), we show four views of the Pt_{13} cluster, with the atom numbers on the atoms (represented by spheres). The colors of the atoms represent their values of Δn_e and d_c values, according to the color bars. Surface-induced electron excess $[\Delta n_e[Pt_{13}] > 0]$ is in blue and depletion $[\Delta n_e[Pt_{13}] < 0]$ in red; neutral atoms are represented by white colored spheres. The value of d_c is calculated relative to the Fermi energy set at 0. For each property we show two views: i) two top views: with only the atoms in the bottom layer of the cluster, in contact with the surface, shown on the left and all the atoms of the cluster shown on the right), and ii) to tilted views, with the ones on the left and right as in (i). Yellow spheres represent Si atoms and small deeper red spheres correspond to oxygen atoms. The underlying lilac spheres depict the Pt(111) substrate. In (b), atoms with particularly larger shifts from the Fermi level (more negative d_c values) are: number 2 ($d_c = -2.78$ e), 4 ($d_c = -2.88$ e), 6 ($d_c = -2.81$ e), 9 ($d_c = -2.57$ e), 10 ($d_c = -2.52$ e), and 12 ($d_c = -2.97$ e).

adsorbed on a-SiO_2 (see Figures 2 and 3). Our work provides the impetus for further investigations of the effect of support stoichiometry, particularly for more applied reactions, where chemoselectivity and stereoselectivity are additional important factors. This could reveal unexpected strategies to control catalytic performance in the future.

Acknowledgements

A.S.C., M.D.R., F.F.S., and U.H. acknowledge financial support through a DFG Grant (Project He 3454/23-1). B.Y. has been supported by a grant from the Air Force Office of Scientific Research (AFOSR), and U.L. was supported by grant No. FG05-86ER45234 from the Office of Basic Energy Sciences of the US Department of Energy (DOE). Computations were done at the Georgia Tech Center for Computational Materials Science.

Keywords: clusters · density functional calculations · ethylene hydrogenation · platinum · silica support stoichiometry

How to cite: *Angew. Chem. Int. Ed.* **2016**, *55*, 8953 – 8957
Angew. Chem. **2016**, *128*, 9099 – 9103

[1] M. Boudart, *Top. Catal.* **2000**, *13*, 147 – 149.
[2] D. W. Goodman, *J. Phys. Chem.* **1996**, *100*, 13090 – 13102.
[3] G. A. Somorjai, K. McCrea, *Appl. Catal. A* **2001**, *222*, 3 – 18.
[4] *Nanocatalysis* (Eds.: U. Heiz, U. Landman), Springer, Berlin, **2007**.
[5] U. Heiz, A. Sanchez, S. Abbet, W.-D. Schneider, *J. Am. Chem. Soc.* **1999**, *121*, 3214 – 3217.
[6] A. Sanchez, S. Abbet, U. Heiz, W.-D. Schneider, H. Häkkinen, R. N. Barnett, U. Landman, *J. Phys. Chem. A* **1999**, *103*, 9573 – 9578.
[7] W. E. Kaden, T. Wu, W. A. Kunkel, S. L. Anderson, *Science* **2009**, *326*, 826.
[8] Y. Watanabe, *Sci. Technol. Adv. Mater.* **2014**, *15*, 063501.
[9] Y. Watanabe, X. Wu, H. Hirata, N. Isomura, *Catal. Sci. Technol.* **2011**, *1*, 1490.
[10] D. Ricci, A. Bongiorno, G. Pacchioni, U. Landman, *Phys. Rev. Lett.* **2006**, *97*, 036106.
[11] C. Zhang, B. Yoon, U. Landman, *J. Am. Chem. Soc.* **2007**, *129*, 2228 – 2229.
[12] C. Harding, V. Habibpour, S. Kunz, A. N.-S. Farnbacher, U. Heiz, B. Yoon, U. Landman, *J. Am. Chem. Soc.* **2009**, *131*, 538 – 548.
[13] M. Sterrer, T. Risse, M. Heyde, H.-P. Rust, H.-J. Freund, *Phys. Rev. Lett.* **2007**, *98*, 206103.
[14] T. Risse, S. Shaikhutdinov, N. Nilius, M. Sterrer, H.-J. Freund, *Acc. Chem. Res.* **2008**, *41*, 949 – 956.
[15] M. D. Kane, F. S. Roberts, S. L. Anderson, *J. Phys. Chem. C* **2015**, *119*, 1359 – 1375.
[16] B. Yoon, U. Landman, A. S. Woerz, J.-M. Antonietti, S. Abbet, K. Judai, U. Heiz, *Science* **2005**, *307*, 403.
[17] S. Bonanni, K. Aït-Mansour, W. Harbich, H. Brune, *J. Am. Chem. Soc.* **2012**, *134*, 3445 – 3450.
[18] *Modern Surface Organometallic Chemistry* (Eds.: J.-M. Basset, R. Psaro, D. Roberto, R. Ugo), Wiley-VCH, Weinheim, **2009**.
[19] G. Ertl, H. Knözinger, F. Schüth, J. Weitkamp, *Handbook of Heterogeneous Catalysis*, *2nd ed.*, Wiley-VCH, Weinheim, **2008**.
[20] Y. D. Kim, T. Wei, D. W. Goodman, *Langmuir* **2003**, *19*, 354 – 357.
[21] Y. D. Kim, T. Wei, S. Wendt, D. W. Goodman, *Langmuir* **2003**, *19*, 7929 – 7932.
[22] C. S. Ewing, M. J. Hartmann, K. R. Martin, A. M. Musto, S. J. Padinjarekutt, E. M. Weiss, G. Veser, J. J. McCarthy, J. K. Johnson, D. S. Lambrecht, *J. Phys. Chem. C* **2015**, *119*, 2503 – 2512.
[23] G. Pacchioni, *Phys. Chem. Chem. Phys.* **2013**, *15*, 1737 – 1757.
[24] J. Horiuti, K. Miyahara, *NSRDS-NBS* **1968**, *13*, 1.
[25] F. Zaera, G. A. Somorjai, *J. Am. Chem. Soc.* **1984**, *106*, 2288.
[26] R. D. Cortright, S. A. Goddard, J. E. Rekoske, J. A. Dumesic, *J. Catal.* **1991**, *127*, 342 – 353.
[27] P. S. Cremer, X. Su, Y. R. Shen, G. A. Somorjai, *J. Am. Chem. Soc.* **1996**, *118*, 2942.
[28] R. M. Rioux, H. Song, J. D. Hoefelmeyer, P. Yang, G. A. Somorjai, *J. Phys. Chem. B* **2005**, *109*, 2192.
[29] H. Song, R. M. Rioux, J. D. Hoefelmeyer, R. Komor, K. Niesz, M. Grass, P. Yang, G. A. Somorjai, *J. Am. Chem. Soc.* **2006**, *128*, 3027 – 3037.
[30] A. S. Crampton, M. D. Rötzer, C. J. Ridge, B. Yoon, F. F. Schwein- berger, U. Landman, U. Heiz, *Surf. Sci.* **2016**, in press, DOI: 10.1016/j.susc.2016.02.006.
[31] A. S. Crampton, M. D. Rötzer, C. J. Ridge, F. F. Schweinberger, U. Heiz, B. Yoon, U. Landman, *Nat. Commun.* **2016**, *7*, 10389.
[32] U. Heiz, F. Vanolli, L. Trento, W.-D. Schneider, *Rev. Sci. Instrum.* **1997**, *68*, 1986 – 1994.
[33] A. S. Crampton, C. J. Ridge, M. D. Rötzer, G. Zwaschka, T. Braun, V. D'Elia, J.-M. Basset, F. F. Schweinberger, S. Günther, U. Heiz, *J. Phys. Chem. C* **2015**, *119*, 13665 – 13669.
[34] K. Judai, S. Abbet, A. S. Wörz, M. A. Röttgen, U. Heiz, *Int. J. Mass Spectrom.* **2003**, *229*, 99 – 106.
[35] C. Harding, S. Kunz, V. Habibpour, V. Teslenko, M. Arenz, U. Heiz, *J. Catal.* **2008**, *255*, 234 – 240.
[36] C. H. Hu, C. Chizallet, C. Mager-Maury, M. Corral-Valero, P. Sautet, H. Toulhoat, P. Raybaud, *J. Catal.* **2010**, *274*, 99 – 110.
[37] J. Chatt, L. A. Duncanson, *J. Chem. Soc.* **1953**, 2939 – 2947.
[38] M. Dewar, *Bull. Soc. Chim.* **1951**, *18*, C71 – C79.
[39] V. Pallassana, M. Neurock, *J. Catal.* **2000**, *191*, 301 – 317.
[40] A. S. Crampton, M. D. Rötzer, F. F. Schweinberger, B. Yoon, U. Landman, U. Heiz, *J. Catal.* **2016**, *333*, 51 – 58.
[41] M. Salmeron, G. A. Somorjai, *J. Phys. Chem.* **1982**, *86*, 341.
[42] T. A. Land, T. Michely, R. J. Behm, J. C. Hemminger, G. Comsa, *J. Chem. Phys.* **1992**, *97*, 6774 – 6783.
[43] M. J. Lundwall, S. M. McClure, D. W. Goodman, *J. Phys. Chem. C* **2010**, *114*, 7904.
[44] R. M. Rioux, J. D. Hoefelmeyer, M. Grass, H. Song, K. Niesz, P. Yang, G. A. Somorjai, *Langmuir* **2008**, *24*, 198 – 207.

Received: April 5, 2016
Published online: June 29, 2016

